Journal of Colloid and Interface Science **217,** 146–153 (1999)
Article ID jcis.1999.6364, available online at http://www.idealibrary.com on IDEAL®

The Directional Dependence of Water Penetration into Langmuir–Blodgett Multilayers

K. P. Girard,* J. A. Quinn,* and T. K. Vanderlick†,[1]

*University of Pennsylvania, Department of Chemical Engineering, Philadelphia, Pennsylvania 19104; and †Princeton University, Department of Chemical Engineering, Princeton, New Jersey 08544

Received February 4, 1999; accepted May 28, 1999

The relationship between the mass uptake and the swelling of arachidic acid Langmuir–Blodgett (LB) films exposed to water vapor was investigated. Combining sorption data from the quartz crystal microbalance with swelling data from the surface forces apparatus (SFA), it was found that films exposed to water vapor (≈75% RH) absorb 0.22 moles water/mole LB film with an associated swelling of 0.2 Å/film layer. This degree of film swelling is less than that predicted if the water taken up exhibits the molar volume of bulk liquid water. The configuration of the films in the SFA, where they are trapped between impermeable surfaces, makes possible the measurement of the lateral diffusion coefficient of water in these layered materials. This was found to be 1.5 × 10^{-10} cm^2/s, which is at least 100 times faster than diffusion normal to the layers as measured with the microbalance. © 1999 Academic Press

Key Words: **Langmuir–Blodgett films; lateral diffusion; water; fatty acid; SFA; QCM.**

INTRODUCTION

Invented over 60 years ago (1), Langmuir–Blodgett films continue to attract attention because of their interesting structure, properties, and processing attributes (2). It is perhaps the latter which underpins the potential of these materials in various applications, as the building process—the creation and addition of one molecular layer at a time—offers both flexibility and control at the nanoscopic level. It is a process based on a synergistic combination of self assembly and human assembly with the associated advantages of each.

The most prevalent structure of LB films is a stack of bilayers, each distinguished by hydrophilic headgroup regions which border juxtaposed hydrophobic alkane tail regions. Akin to biological bilayers, this basic substructure makes LB films candidates for models of natural membranes (3). More generally, the highly stratified and internally contrasting nature of these films may impart them with unique, anisotropic, and controllable properties, including, and especially, permeability. Indeed, one potential application of LB films is in membrane-based separations (4, 5).

[1] To whom correspondence should be addressed.

The uptake of water into LB films is significant for reasons beyond the scenario of using LB films in barrier or membrane applications. The response of these materials to humidity, for example, may compromise their performance in various optical and electrical applications where precise control of film thickness and/or dielectric constant is required. Born from the surface of water, LB films interact with this most ubiquitous fluid in ways that impact their growth, reflect their structure, and determine their stability.

The most extensively studied LB films are those composed of fatty acids and their divalent metal salts. Although the ion type and composition of these films can vary, for brevity we refer to them simply as fatty acid films. By forming films on a quartz crystal microbalance (QCM), it has been possible to study quantitatively the transport of water in and out of these LB films. In this way, Ariga *et al.* (6) and later Lovell *et al.* (7) measured the evaporation rate of water entrained during deposition. Hanley *et al.* (8) used this technique to study water vapor sorption as a function of vapor pressure. Spectroscopic measurements offer another route to study water uptake. Marshbanks *et al.* (9) used infrared spectroscopy (FTIR) to study diffusion of water into films immersed in a water bath. All of these studies confirm that transport of water through these well-ordered, densely packed films is slow, with apparent diffusion coefficients ranging from 10^{-9} cm^2/s (7) to as low as 5×10^{-13} cm^2/s, (9) with typical values hovering about 10^{-12} cm^2/s (6, 8).

The geometric nature of all these experiments is similar and lends itself to the study of permeation vertically through the film, that is, normal to the molecular layers. Attempts to describe the rate of water loss (or gain) using a Fickian model for one-dimensional transport in this direction (7, 9) do not match most experimental findings. Different explanations have been put forward to account for this behavior. For example, Lovell *et al.* (7) propose two parallel pathways for transport: one cutting through behenic acid regimes characterized by a diffusion coefficient of 1×10^{-10} cm^2/s and one through behenic acid salt regimes with a slightly faster diffusivity of 1×10^{-9} cm^2/s. Marshbanks *et al.* (9) suggest that the transport is not purely one-dimensional and that lateral transport near

0021-9797/99 $30.00

defects within the film may contribute to the observed behavior.

As far as water content is concerned, fatty acid LB films can contain as much as 50 wt% water as a result of entrainment during deposition (6) and as little as none for a pure acid film in a dry environment (9). Using FTIR, Marshbanks *et al.* (9) found that calcium stearate films in ambient conditions contain 2.7 wt% water. These same films take up an additional 13 wt% (2.6 moles water/mole film) when contacted with liquid water. By careful analysis of their spectra, they concluded that the additional mass of water in the film does not result in any structural change. Upon drying these films, the residual water content drops to about 1.2 wt%. Using the QCM, Hanley *et al.* (8) showed that behenic acid/salt films pick up about 1.5 wt% water as the vapor pressure is increased from zero to near saturation.

A completely different approach to studying the interaction of water with LB films is to probe their swelling phenomena, i.e., changes in thickness due to water gain or loss. Using X-ray scattering Höhne and Möhwald showed that magnesium stearate films swelled by 3 Å per bilayer when taken from a dessicated, reduced pressure environment and rehydrated by liquid water (10). Rapp *et al.* (11) also studied the bilayer spacing of magnesium stearate. With time-resolved X-ray diffraction this group showed the bilayer spacing to decrease by 3 Å when heated above 50°C. Based on the sum of the correlation lengths of the respective diffracting units, they concluded this decrease in thickness was due to the loss of water through defects in the film.

The link between mass uptake and associated swelling is interesting and currently unknown. In the language of thermodynamics, the partial molar volume of water dissolved in LB films is undetermined. It is not obvious that this should equal the molar volume of bulk liquid water: adsorbed water which does indeed add volume to the film may not behave at all like bulk water. Moreover, the presence of free volume, holes, and/or gross defects in the film may allow water to be picked up without any significant swelling.

One may try to establish a connection between mass uptake and associated swelling by piecing together available experimental data, but the conclusions would be tentative given the variability of parameters and systems. One can compare, for example, the swelling observed by Höhne *et al.* (10) with the water content measurements reported by Marshbanks *et al.* (9). The latter researchers found that films contacted by liquid water picked up 15 wt% water. Assuming this same amount of water causes the swelling observed by Höhne leads to an effective partial molar volume of water equal to half that of bulk water. Or, assuming instead that the partial molar volume of water is that of bulk liquid leads to the conclusion that water solubility in Höhne's magnesium stearate films is roughly half of that in Marshbanks' calcium stearate films. This difference might simply reflect the different hydration tendencies of the two metal cations.

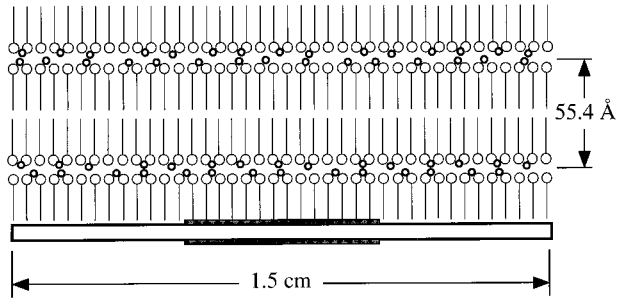

FIG. 1. Quartz Crystal Microbalance crystal coated by an LB film with included cations. Only the area where the electrodes overlap is sensitive to mass absorbed. Self-assembled monolayers used to make the gold and quartz hydrophobic as well as the film deposited on the bottom face of the crystal are not shown for clarity. Bilayer thickness is 55.4 Å determined with our SFA.

In this work, we use a combination of two tools to accomplish two objectives. The swelling of fatty acid films upon exposure to water vapor is measured using the capabilities of the surface forces apparatus (SFA); the mass uptake in similarly prepared films is determined using a quartz crystal microbalance. The two measurements establish a quantitative link between mass uptake and associated thickness change. Second, and perhaps more importantly, the geometric nature of the surface forces experiment lends itself to probing transport mainly along the layers of the film, since the film is sandwiched between two impermeable surfaces made of mica. Hence the lateral transport rate determined from the kinetics of film swelling can be compared to the rate of transport normal to the film as measured with the QCM.

BACKGROUND: ESTABLISHING PENETRATION GEOMETRIES

The QCM is a piezoelectric sensor with nanogram sensitivity to mass changes on its surface. More specifically, the device is only sensitive to mass adsorbed onto the area where the electrodes overlap (see Fig. 1). The principles and operation of the device are described in detail elsewhere (12, 13). As shown in Fig. 1, this geometric configuration lends itself to measurements of water penetration in a normal direction, that is, parallel to the chains of the LB film which is built on the QCM surfaces. The transport geometry is that of a plane sheet with no flux boundaries at the crystal faces. Assuming purely one-dimensional transport (infinite planar sheets) and Fickian diffusion kinetics results in the following governing equation for mass pick-up (14)

$$\frac{M(t)}{M(\infty)} = 2\left(\frac{Dt}{l^2}\right)^{1/2}\left\{\pi^{1/2} + 2\sum_{n=1}^{\infty}(-1)^n \,\mathrm{ierfc}\,\frac{nl}{\sqrt{Dt}}\right\}, \quad [1]$$

where $M(t)$ is the mass of water in the film at any time, $M(\infty)$

is the mass of water in the film at equilibrium, D is the diffusion coefficient, t is time, and l is the film thickness.

The SFA is a tool designed to measure the force acting between opposed surfaces as a function of their separation (15–17). It is equally well suited for studies of adhesion and associated deformations of surfaces in contact (18, 19). The SFA has been used to investigate a wide variety of interfacial systems (20, 21), including monolayers and bilayers produced by LB deposition (22, 23). Central to SFA measurements is the application of multiple beam interferometry to determine relevant distances, e.g., surface separations or film thickness. In fully optimized conditions, this can be achieved with angstrom-level resolution.

Molecularly smooth mica sheets are typically employed in the SFA, and these are glued onto gently curved ($R \approx 1$ cm), cylindrically shaped support lenses. When these smooth, curved bodies are brought into contact with each other, they deform about the initial point of contact to produce a finite area of intimate contact. The size of this area depends on the effective modulus of the system as well as the magnitudes of externally applied loads and adhesive forces; the shape of the contact area is dominated by the bulk geometry. The geometry of opposing crossed-cylinders used in the SFA is, to first-order approximation, equivalent to that of a sphere and a plane. Thus the resulting area of intimate contact is flat and of circular shape, similar to that which would be generated when a soft sphere is pressed against a hard surface. In a typical SFA experiment, the size of flattened contact is 30–100 μm in diameter.

We take advantage of this flattening to carefully sandwich LB multilayers between two impermeable mica sheets. An LB film is built upon one of the two mica surfaces which are then loaded into the SFA. Using interferometry to accurately measure the separation between the two bodies, we bring the surfaces progressively closer until they (unavoidably) jump into adhesive contact, effectively capping the film at its top and bottom across the region of intimate contact, as shown in Fig. 2. Interferometry is then used to measure the thickness of the film as it responds to deliberate changes in humidity.

Note that water must first permeate vertically through the film at and beyond the perimeter of the contact region, then diffuse through the LB film primarily in the lateral direction. Since the film is extremely thin, the vertical transport is very fast compared to the lateral transport, which is characterized by a length scale associated with the area of contact. The geometry of transport into the capped film can be approximated as one-dimensional radial diffusion into a cylinder. The corresponding governing equation for Fickian diffusion is (14)

$$\frac{M(t)}{M(\infty)} = \frac{4}{\pi^{1/2}}\left(\frac{Dt}{a^2}\right)^{1/2} - \frac{Dt}{a^2} - \frac{1}{3\pi^{1/2}}\left(\frac{Dt}{a^2}\right)^{3/2} + \cdots, \quad [2]$$

where a is the radius of the cylinder.

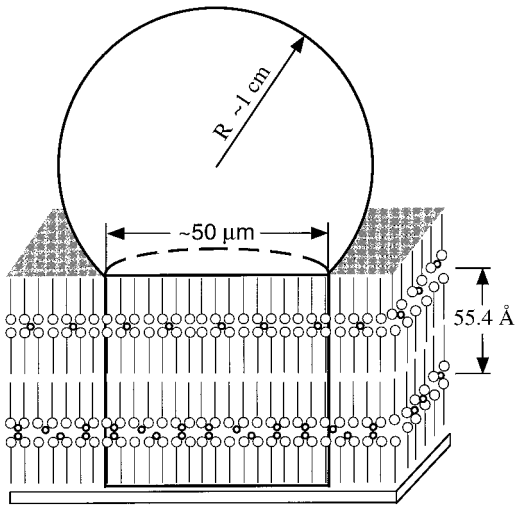

FIG. 2. Cross-section view of the local SFA geometry showing an LB film sandwiched between two smooth surfaces. Flattening about the initial point of contact traps a cylidrical volume of LB film which cannot be penetrated from above or below.

EXPERIMENTAL

Materials Details

Arachidic acid, subphase salts ($BaCl_2$, $KHCO_3$, and $CuCl_2$), octadecyl mercaptan, and octadecyltrichlorosilane (OTS) were of the highest grade available, purchased from Sigma (St. Louis, MO) and used as received. HPLC chloroform and methanol for spreading solutions were purchased from Fisher (Pittsburgh, PA). Dipalmitoylphosphatidylethanolamine (DPPE) was purchased from Avanti Polar Lipids (Alabaster, AL) and used without further purification. Water used as a subphase in the depositions was produced by a Milli-Q unit and had a resistivity of 18 MΩ/cm. The arachidic acid LB multilayers used in this study were prepared on either quartz microbalance crystals supplied by Classic Frequency Control (Oklahoma City, OK) or freshly cleaved mica supplied by Mica New York (New York, NY). The Langmuir trough and dipping device was automated and built by KSV Instruments (Finland).

Arachidic acid LB films were deposited from an aqueous subphase containing 10^{-4} M $BaCl_2$, and 2×10^{-4} M $KHCO_3$ and held constant at 20°C. The $KHCO_3$ buffered the subphase to a pH of 6.5. $CuCl_2$ was added to the subphase until its final concentration was 4×10^{-7} M; this concentration has been shown to aid the deposition of large numbers of layers (24). Monolayers were spread from an $\approx$1 mg/ml solution of fatty acid and chloroform, the latter being allowed to evaporate for 10 min before compressing the monolayer to 30 mN/m. Once this pressure was reached, the films were allowed 15 min to stabilize before conventional dipping commenced at a speed of 10 mm/min. At least 5 min elapsed between the upstroke and the downstroke to allow entrained subphase to evaporate and to enhance further transfer. Transfer ratios were always 0.95 to

1.02 as measured by both barrier movement and dry film weight.

QCM Details

The QCM consisted of a homemade oscillator circuit, a removable quartz crystal, and an HP5334B frequency counter (Hewlett Packard, Rockville, MD). Electrodeless 10-MHz crystals with 0.3 μm average roughness were chemically cleaned by the RCA method (25) before being made hydrophobic with OTS (26). Gold electrodes were then evaporated onto the quartz and made hydrophobic using octadecyl mercaptan. The baseline frequency in air (stable to $\pm$ 0.5 Hz) was noted before various numbers of LB layers were deposited on the crystal as described above.

Following deposition, the crystal frequency was again noted so that the dry film weight could be calculated. The equilibrium and kinetics of water sorption were then measured in a vacuum system similar to that used by others to study vapor transport in polymers (27). The films are initially evacuated to less than 30 mTorr and the baseline frequency of the QCM is noted. A controlled amount of vapor ($P/P_o = 0.6$) is introduced into the chamber while the frequency change, and thus the mass pickup, is recorded with a computer as time progresses.

SFA Details

Mica was freshly cleaved, cut with a hot platinum wire, and silvered with 480 Å on one side by thermal evaporation. The surfaces were then glued, silver side down, to silica disks and one surface was made hydrophobic by a monolayer of DPPE before depositing the arachidic layers. The phospholipid monolayer was deposited using the same conditions as Marra (22) and was allowed to dry for at least 10 min while changing to the salt subphase. Subsequent layers of arachidic acid were deposited onto the hydrophobic mica as described above.

The LB-coated surface was placed into the SFA with an opposing mica surface and was dried, out of contact, by evacuating the space within the SFA using a vacuum system identical to that used with the QCM. The dry surfaces were brought into molecular contact and the positions of the interference fringes were noted by recording them with a CCD camera. Humidity was controlled with vials of saturated NaCl solution or by evacuation with a vacuum pump. The shifts of the interference fringes were monitored by taking CCD images at regular intervals with an optical detection system previously described by Levins *et al.* (28). The equations put forth by Israelachvili (29) were used to determine the film thickness from the interferometric measurements.

RESULTS AND DISCUSSION

A complication immediately arises in both QCM and SFA experiments: namely, distinguishing from the total signal the part due to mass absorption (i.e., film solubility) and that due to mass adsorption at the various material interfaces that may be present. Fortunately, the integral nature of LB films can be exploited to identify these individual contributions (8). In particular, data is collected from a series of films differing only by their number of constituent layers. A plot of mass uptake (or total swelled amount) versus the number of layers yields a slope corresponding to the solubility of water, i.e., mass absorbed per layer (or average swelling per layer). Meanwhile, the intercept at zero layers provides a measure of mass adsorbed at the system interfaces.

We found this strategy critical for experiments carried out in the surface forces apparatus since we found it difficult to build good quality films beyond about 30 layers on the curved supports used in the apparatus. The expected jump into contact was often not observed for thicker films, indicative of impurities and/or severe film disruption. It was, however, quite easy to build up to a hundred layers atop a silanized quartz crystal used for mass sorption measurements.

While the strategy discussed above was indeed used to determine the swelling due solely to water absorbed, we took extra precaution to minimize the amount of water likely to be adsorbed. In particular, instead of depositing the fatty acid molecules directly onto hydrophilic mica, we first deposited a single layer of the phospholipid DPPE. We performed experiments with this monolayer in the SFA and found that DPPE trapped between mica sheets and exposed to humid air swelled, typically 2 Å in going from 0 to 75% relative humidity (RH). Using the SFA, Chen *et al.* (23) studied the humidity response of DMPE, a similar molecule, and found that the thickness of DMPE changed by less than 1 Å over the entire humidity range. Thus we can be assured the swelling due to adsorption at the phospholipid/mica interface will be minimal.

Equilibrium Mass Uptake and Swelling

The equilibrium amount of water vapor sorbed by arachidic acid LB films of various thickness as measured with the QCM is shown in Fig. 3. Water uptake increases linearly with the number of film layers; the slope yields a molar solubility of 0.2 moles water per mole LB film ($\approx$0.8 wt%) and is in excellent agreement with work done previously in our lab by Hanley *et al.* (8) who also reported a solubility of 0.2 moles/mole. Our solubility, measured at $P/P_o = 0.6$, also agrees well with the findings of Marshbanks *et al.* (9) who reported their stearic acid films to retain $\approx$1.4 wt% water (0.23 moles/mole) in ambient air, which typically contains 60–70% relative humidity.

The nonzero intercept of the best-fit line in Fig. 3 represents water adsorbed at the system's interfaces, i.e., at the QCM/film interface and/or the film/air interface. This amount of water, 3.4×10^{-8} g/cm^2, is equivalent to 1.4 monolayers water or 3.3 Å. An ellipsometric study by Tadros *et al.* (30) provides some insight as to the location of our adsorbed water. They found that a water layer 4 Å thick adsorbs to the stearic acid/air

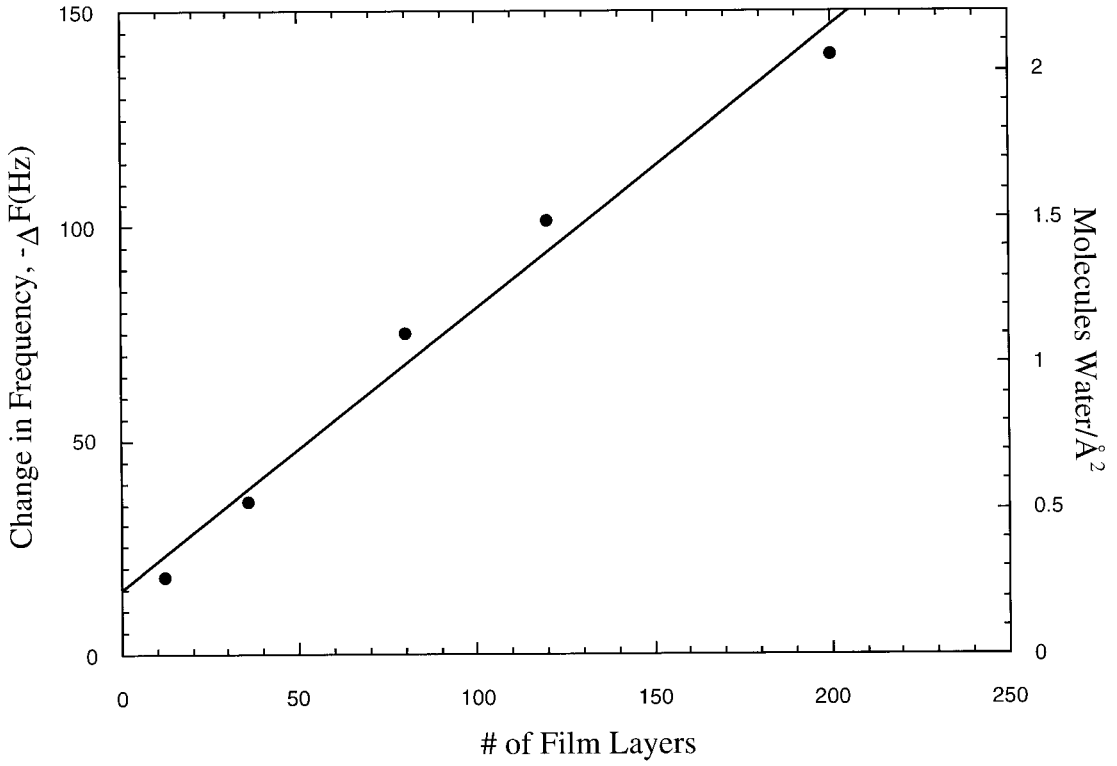

FIG. 3. Equilibrium mass uptake of water vapor at $P/P_o = 0.6$ by arachidic acid LB films of increasing thickness as measured with the QCM. The slope of the line is 0.66 Hz/layer which yields a solubility of 0.2 moles water/mole film. The intercept gives an estimate of surface adsorption which is ≈3 Å.

interface of a monolayer exposed to humid atmosphere ($P/P_o = 0.7$). Our measured adsorption agrees well with this finding, and thus it is likely that the water adsorbed on our films is located mainly at the film/air interface.

Before discussing the swelling data, the rationale for using slightly different vapor pressures with the QCM and SFA experiments should be explained. The QCM experiments were performed first and were conducted at $P/P_o = 0.6$. Humidity in the SFA was controlled using salt solutions, and we chose the readily available NaCl, which yields a relative humidity of 75%. Hanley (8), however, studied the relationship between vapor pressure and solubility and found that films exposed to $P/P_o = 0.75$ pick up about 10% more mass than those exposed to $P/P_o = 0.6$. Hence, we use a solubility of 0.22 moles/mole (instead of 0.2 moles/mole) as a benchmark for comparing the mass uptake with swelling results below.

The change in thickness of the fatty acid films, as measured in the SFA, upon equilibration with air containing 75% RH (starting or ending in vacuum) is shown in Fig. 4. The signal to noise ratio for these experiments is much lower than for the QCM because we were restricted to thinner films in the SFA. Typically, SFA experiments afford angstrom- and even sub-angstrom-level resolution of film thickness, especially when considering changes in film thickness. Our estimated error is somewhat larger than this, most probably due to our difficulty in establishing and controlling humidity in the SFA. We estimate our error to be ±1.2 Å, as based on our repeat experiment with a 10-layer film.

Fitting the data with a least-squares line yields a slope of 0.2 Å per layer and a surface adsorption of about 3 Å. This surface adsorption is about what we would expect given our independent measurements with DPPE/mica interfaces. It is also clear that the hydrocarbon interfaces of the LB film, whether in contact with hydrophobic air or hydrophilic mica, do not adsorb more than a few angstroms of water, i.e., less than a monolayer.

The results of the two techniques can now be brought together. To do so, we assume that the LB films formed on SFA substrates absorb the same amount of water per layer as those formed on the QCM; apart from effects due to confinement (which will be discussed later) there are no obvious reasons why this should not be valid. In this case, 0.22 moles water/mole LB film is associated with a swelling of 0.2 Å per layer. If the partial molar volume of water is taken to be that of bulk liquid water, the amount of water absorbed would cause a swelling of about 0.3 Å per layer; this is 0.1 Å per layer more than what is observed. This suggests that either some water is filling defects or holes with little or no bearing on thickness, and/or that water taken up within the film (probably located within the headgroup regions) is in a state unlike that of bulk water. Both possibilities are likely and our results cannot distinguish between the two.

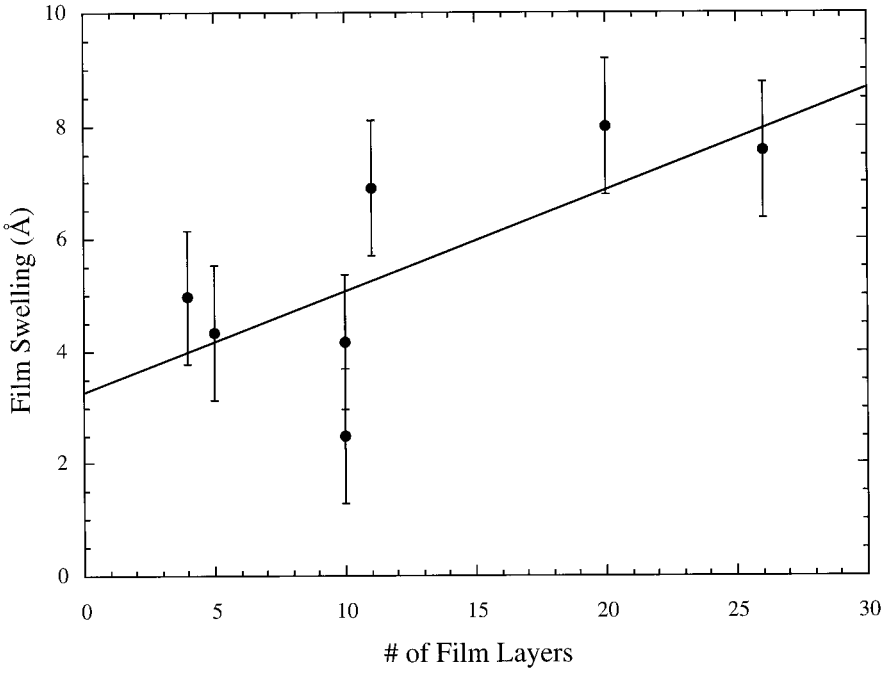

FIG. 4. Equilibrium swelling of arachidic acid LB films due to water vapor uptake at 75% relative humidity as measured with the SFA. The slope of the line gives the swelling per layer (0.2 Å/layer), and the intercept gives the swelling due to adsorption at the interfaces of the system. (≈3 Å)

It is also possible that the LB films in the SFA are characterized by a lower water solubility as a result of confinement. A contact mechanics analysis (31) reveals that bodies in adhesive contact must support a distribution of stress (both compressive and tensile) within the contact zone, even under zero applied load. At the center of the contact region a reasonable estimate of this stress is of order 10–20 MPa (18). Our measurements, however, reveal no significant differences in thickness across the region of contact. It may be, however, that such differences, if they exist, are beyond the resolution of the interferometric technique.

It may ultimately be possible to establish the effects of confinement on sorption since the SFA can be used to systematically vary the external load transmitted to the surfaces. In these experiments, however, one must also account for the mechanical response of the film itself to applied stress. We are pursuing such measurements and results will be reported in a future publication.

Kinetics of Mass Uptake: Normal and Lateral Diffusion

Figure 5 shows the kinetics of water sorption by arachidic acid LB films as measured with the QCM. Using the initial slope of the curve, we can estimate an upper bound for the diffusion coefficient to be 1×10^{-12} cm^2/s. If we fit the data to Eq. [1], we obtain a diffusion coefficient of 2×10^{-13} cm^2/s. These results are within the range cited by Marshbanks *et al.* (9) and compare well with the diffusion coefficient cited by Ariga (6), 9×10^{-12} cm^2/s. Our rates are slightly slower than those reported by Lovell *et al.* (7); however, our films are significantly drier and thus perhaps more solid-like than their freshly prepared films.

The extremely slow diffusion was an expected result, since penetration should be greatly impeded by the solid-like film. Resistance to mass transport is high, since permeation through the tightly packed, hydrophobic chains is unfavorable for water molecules. It is also clear from the data that the penetration is not purely Fickian. As discussed above, others have proposed theories to better model the system by accounting for its anisotropy. Nevertheless, the apparent diffusion coefficient obtained from the simple Fickian model provides a reasonable estimate that can be contrasted with the kinetics of film swelling as observed in the SFA.

The swelling kinetics of films exposed to water vapor in the SFA are shown in Fig. 6. The solid line shown is a fit to the data using the Fickian model for radial diffusion into a cylinder, Eq. [2]. Although the data do not strictly follow one-dimensional Fickian kinetics, the fit agrees well enough to yield a diffusion coefficient of 1.5×10^{-10} cm^2/s. Similar experiments conducted on films of various thickness and for both dosing and evacuation have yielded transport curves with diffusion coefficients as large as 1.7×10^{-9} cm^2/s and as small as that quoted above. We find that lateral diffusion is at least two orders of magnitude faster than diffusion of water in the normal direction, as determined using the QCM. Clearly, the resistance to mass transfer in the lateral direction is less. This may simply reflect that fact that water transported in this

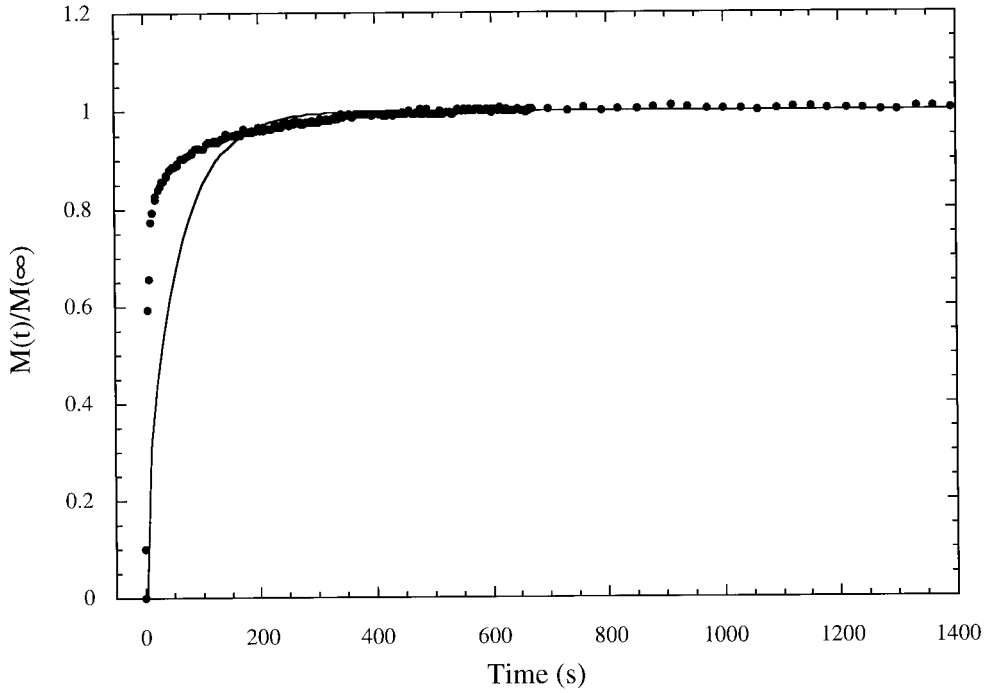

FIG. 5. Kinetics of water vapor sorption by arachidic acid LB films at $P/P_o = 0.6$ as measured with the QCM. The solid line is a fit to the data using a one dimensional model of Fickian diffusion into a plane sheet ($D = 2 \times 10^{-13}$ cm^2/s).

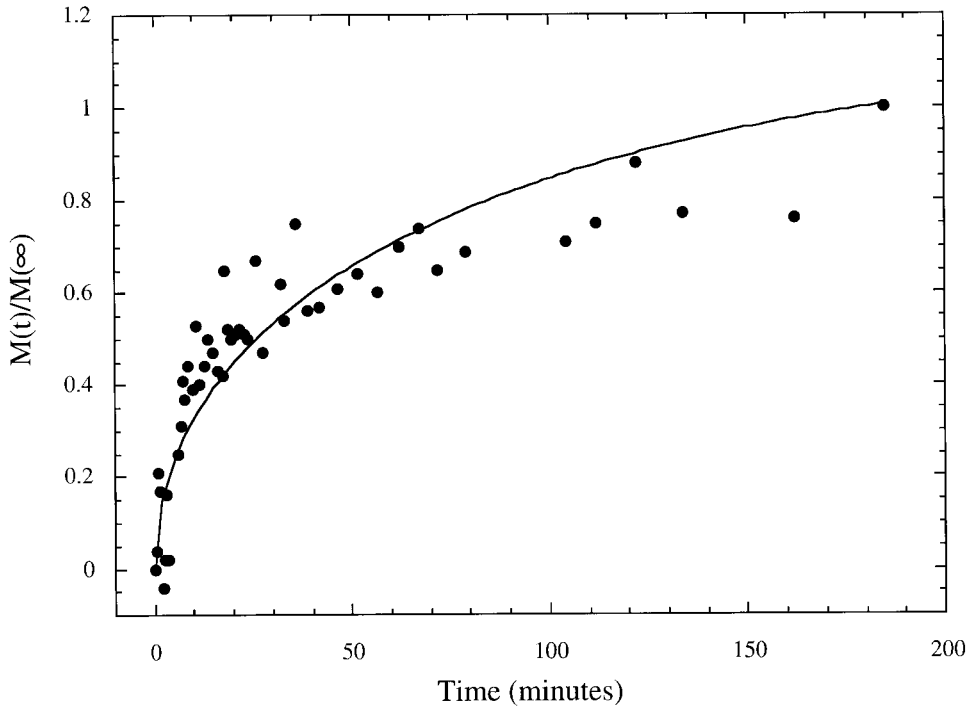

FIG. 6. Kinetics of water vapor sorption by arachidic acid LB films at 75% relative humidity as measured with the SFA. Fractional mass uptake is assumed equivalent to the fractional thickness change measured by interferometry. The solid line is a fit to the data using a one dimensional model of Fickian diffusion into a cylinder ($D = 7 \times 10^{-10}$ cm^2/s).

direction is not limited by diffusion through the close-packed hydrophobic tails.

It is also important to note the difference in time scales displayed in Figs. 3 and 4. Even though the normal diffusion coefficient is much smaller than the lateral diffusion coefficient, the permeability of transport normal to the film is much higher, as the characteristic length is small, around 500 Å. By contrast, the relevant length scale for radial diffusion is on the order of 20–30 μm.

CONCLUSIONS

This work has shown how the combination of the QCM and the SFA can be used to link the mass uptake of water vapor by LB films to the associated swelling. The degree of film swelling is less than that predicted if the water taken up exhibits the molar volume of bulk liquid water. This difference may be attributed to a number of factors, including the filling of voids or defects as well as the nonbulk nature of sorbed water. Confinement may also play a role, perhaps by reducing the solubility of water in the film. The kinetics of water sorption in the vertical (normal) and lateral directions were contrasted. It was found that lateral diffusion is at least 100 times faster than vertical diffusion, typical values being 1.5×10^{-10} and 1×10^{-12} cm^2/s, respectively.

ACKNOWLEDGMENT

We gratefully acknowledge the support for this work provided by the National Science Foundation (Grant CTS-9615868).

REFERENCES

1. Blodgett, K. B., *J. Am. Chem. Soc.* **57,** 1007 (1935).
2. Roberts, G. (Ed.), "Langmuir–Blodgett Films." Plenum Press, New York, 1990.
3. Sackmann, E., *Science* **271,** 43 (1996).
4. Rose, G. D., and Quinn, J. A., *J. Colloid Interface Sci.* **27,** 193 (1968).
5. Maximychev, A. V., Matyukhin, V. D., Stepina, N. D., and Yanusova, L. G., *Thin Solid Films* **285,** 866 (1996).
6. Ariga, K., and Okahata, Y., *Langmuir* **10,** 3255 (1994).
7. Lovell, M. R., and Roser, S. J., *Langmuir* **12,** 2765 (1996).
8. Hanley, C. M., Quinn, J. A., and Vanderlick, T. K., *AICHE J.* **42,** 1234 (1996).
9. Marshbanks, T. L., Ahn, D. J., and Franses, E. I., *Langmuir* **10,** 276 (1994).
10. Höhne, U., and Möhwald, H., *Thin Solid Films* **243,** 425 (1994).
11. Rapp, G., Koch, M. H. J., Höhne, U., Lvov, Y., and Möhwald, H., *Langmuir* **11,** 2348 (1995).
12. Buttry, D., and Ward, M., *Chem. Rev.* **92,** 1355 (1992).
13. Ballantine, D. S., White, R. M., Martin, S. J., Ricco, A. J., Zellers, E. T., Frye, G. C., and Wohltjen, H., "Acoustic Wave Sensors: Theory, Design, and Physico-Chemical Applications." Academic Press, New York, 1997.
14. Crank, J., "The Mathematics of Diffusion (Second Edition)." Clarendon Press, Oxford, 1975.
15. Tabor, D., and Winterton, R. H. S., *Proc. R. Soc. London. Series A. Math. Phys. Sci.* **312,** 435 (1969).
16. Israelachvili, J. N., and Tabor, D., *Proc. R. Soc. London. Series A. Math. Phys. Sci.* **331,** 19 (1972).
17. Israelachvili, J. N., and Adams, G. E., *J. Chem. Soc. Faraday Trans. I* **74,** 975 (1978).
18. Horn, R. G., Israelachvili, J. N., and Pribac, F., *J. Colloid Interface Sci.* **115,** 480 (1987).
19. Levins, J. M., and Vanderlick, T. K., *J. Phys. Chem.* **99,** 5067 (1995).
20. Israelachvili, J. N., and McGuiggan, P. M., *Science* **241,** 795 (1988).
21. Israelachvili, J. N., "Intermolecular and Surface Forces (Second Edition)." Academic Press, New York, 1992.
22. Marra, J., and Israelachvili, J. N., *Biochemistry* **24,** 4608 (1985).
23. Chen, Y. L., and Israelachvili, J. N., *J. Phys. Chem.* **96,** 7752 (1992).
24. Blodgett, K. B., *J. Phys. Chem.* **41,** 975 (1937).
25. Kern, W., and Puotinen, D. A., *RCA Rev.* **31,** 187 (1970).
26. Sagiv, J., *J. Am. Chem. Soc.* **102,** 92 (1980).
27. Laatikainen, M., and Lindström, M., *J. Membrane Sci.* **29,** 127 (1986).
28. Levins, J. M., and Vanderlick, T. K., *Langmuir* **10,** 2389 (1994).
29. Israelachvili, J. N., *J. Colloid Interface Sci.* **44,** 259 (1973).
30. Tadros, M. E., Hu, P., and Adamson, A. W., *J. Colloid Interface Sci.* **49,** 184 (1974).
31. Johnson, K. L., "Contact Mechanics." Cambridge Univ. Press, New York, 1985.